Influence of H2O on NO formation during char oxidation of biomass

Karlström, Oskar; Hao, Wu; Glarborg, Peter

Published in:
Fuel

DOI:
10.1016/j.fuel.2018.08.156

Published: 01/01/2019

Document Version
Accepted author manuscript

Document License
CC BY-NC-ND

Influence of H_2O on NO formation during char oxidation of biomass

Oskar Karlström*[a], Hao Wu[b], Peter Glarborg[b]

[a]Johan Gadolin Process Chemistry Centre, Åbo Akademi University, Finland

[b]Department of Chemical and Biochemical Engineering, Technical University of Denmark

*corresponding author, email: okarlstr@abo.fi, address: Piispankatu 8 20500 Turku, Finland

Abstract

The present study investigates conversion of char-N to NO in mixtures of O_2/N_2 and in $O_2/H_2O/N_2$. Biomass particles of spruce bark were combusted in an electrically heated single particle reactor at 900 °C at various $O_2/H_2O/N_2$ concentrations. NO concentrations of the product gases were measured during the char combustion stage. The conversion of char-N to NO was significantly higher with H_2O as compared to without H_2O in the gas. Additional fixed bed experiments were conducted to investigate the products of the reaction between H_2O and spruce bark char. The results showed that NH_3 is the primary product in the reaction between char-N and steam. These results explain the observation that more NO is formed during char combustion in the presence of steam: the char-N reacts partly with H_2O to form NH_3, which reacts further to NO.

Keywords: biomass; char; NO; NH3, gasification, steam gasification, combustion, oxidation

1. Introduction

Combustion and gasification of biomass generate NOx emissions. In combustion and gasification of biomass most of the NOx origins from the fuel bound nitrogen (fuel-N) [1]. Some biomasses such as pine or birch wood have relatively low nitrogen contents [2] while for example algae or many agricultural biomasses have relatively high nitrogen contents [3]. However, because of very strict NO legislations and environmental reasons, even biomasses with low N contents may give rise to too high NOx emissions, requiring expensive cleaning strategies [4]. Around 70-90% of the fuel-N is bound to

the volatile matter (vol-N) and released during devolatilization [2]. The remaining part, around 10-30%, is mostly bound to the char (char-N) [3]. For some biomasses, such as black liquor, the split differs: for black liquor the char-N may account for more than 50% of the fuel-N [5]. During devolatilization, the vol-N reacts to NH_3, HCN, HNCO, NO, N_2O, N_2 and tar-N [6]. The product distribution depends on the nitrogen content of the fuel, volatile matter, heating rate, final temperature, surrounding gas atmosphere, and how the nitrogen is bound to the fuel [1]. During char conversion, char-N reacts with O_2 to NO. The NO formed from the char-N does not, however, correspond to the release of NO from the same char particle, since it can be reduced to N_2 within the pore system [7,8]. Interestingly, the conversion of char-N to NO increases with decreasing particle size [7–10]. This can be explained by the fact that for a small particle more of the initially formed NO diffuse out from the particle resulting in less possibility for intra-particle reduction of NO to N_2 [11]. For coal chars the influence of steam and CO_2 on char-N conversion has been investigated. Park et al. [12] suggested that coal char-N reacts with CO_2 forming N_2, while char-N reacts with H_2O forming NH_3, HCN and N_2. As NH_3 and HCN are NOx precursors [1,13,14], the NOx emissions vary dependent on whether the combustion occurs in O_2/N_2 or in $O_2/CO_2/H_2O/N_2$. In combustion and gasification, the char conversion always occurs in an environment with H_2O and CO_2 present, besides O_2 [15–17].

The present study investigates conversion of biomass char-N to NO in O_2/N_2 and in $O_2/H_2O/N_2$ in a single particle reactor. The biomass which is investigated is spruce bark char. Barks often have relatively high nitrogen contents in comparison to many other biomass fuels. Bark is one of the main residues from the wood and paper industry and is one of the most significant biomasses used in industrial thermal conversion. In addition, fixed bed reactor experiments are performed between H_2O and the bark char in order to quantify the release of NH_3 under steam gasification conditions.

2. Experiments

Experiments were conducted in a single particle reactor (section 2.2) and in a fixed bed reactor (section 2.3). For the single particle reactor experiments, pellets were pressed from spruce bark particles, while in the fixed bed reactor char produced from the spruce bark was used.

2.1 Materials

Samples of spruce bark were ground and sieved to a size fraction of 250–1000 µm. Single particle samples were prepared by pressing 200 mg of parent biomass into cylindrical pellets with a diameter of 8 mm. A single pellet is hereafter referred to as a single particle. The carbon, hydrogen, nitrogen, and sulfur contents of the samples and of the chars were analyzed with a Thermo Scientific Flash 2000 Organic Element Analyzer (Flash 2000) (see Table 1). Chars for elemental analysis were produced by inserting the parent fuel in N_2 and removing the chars after the devolatilization had ended. In the NO release experiments the chars were produced in situ. The metal content of the biomass samples were analyzed by inductively coupled plasma optical emission spectroscopy (ICP-OES) (see Table 2).

Table 1. CNHS of fuel and char.

	wt-% on dry basis					char yield (%)	Ash content (%)
	N	C	H	S	O*		
spruce bark	0.27	46.2	5.8	0.00	43.3	24.9	4.4
spruce bark char	0.32	74.5	0.99	0.00	6.5	100.0	17.7

*by difference

Table 2. Elemental analysis of fuel and char.

	mg/kg (db)											
	Al	Ca	Fe	K	Mg	Mn	Na	P	S	Si	Ti	Zn
spruce bark	206	11499	140	1496	684	610	< 120	297	241	283	5	45
spruce bark char	676	36142	510	4995	2237	1981	< 120	929	278	697	15	< 4

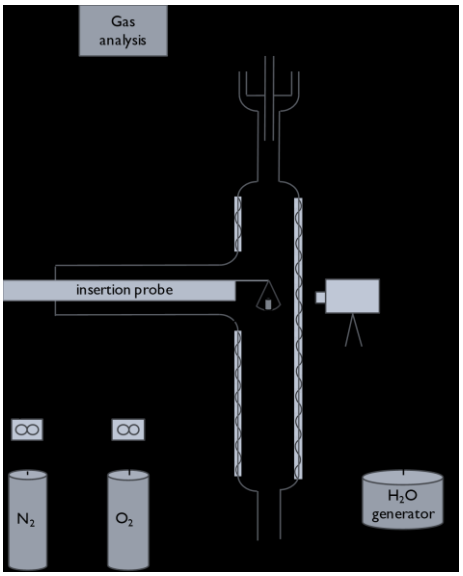

Fig. 1. Single particle reactor for combustion experiments [18].

2.2 Single particle reactor

Experiments were conducted in a single particle reactor at 900 °C in the following gas mixtures with N_2 as the balance gas (% refers here to vol.%): 1% O_2 /14%H_2O, 3% O_2 /14%H_2O, 6% O_2 /14%H_2O, 3% O_2, 6% O_2 and 9% O_2. Chars were produced by inserting the parent fuel in N_2 and removing the chars after the devolatilization had ended.

A detailed description of the reactor can be found elsewhere [18,19]. The single particle reactor consists of a quartz tube reactor inserted in a ceramic furnace. The inner diameter of the tube is 44.3 mm. Gas mixtures of oxygen, nitrogen and steam were fed in the bottom of the reactor and the product gases left from the top of the reactor. Nitrogen was also injected from three sides of the reactor system, on the same level as the particle insertion, to ensure a good mixing of the gases. The biomass sample was inserted into the reactor using a movable horizontal probe that could be inserted from room temperature into the hot reactor within one to two seconds. The sample holder consisted of a thin net on which a single fuel pellet was placed. Concentrations of NO, CO_2 and CO in the outlet gases were continuously measured with a Teledyne Instruments Model 200E and with an ABB AO2020 analyzer. The measuring ranges of the CO and CO_2 analyzers are 0-10%, and the measuring range for

the NOx analyzer is 0-60 ppm. The accuracy of the CO and CO_2 analyzers is 0.01%, while the accuracy of the NO analyzer is 0.1 ppm. The measurement accuracies of the analyzers are those as reported by the analyzer manufacturers. Figure 2 shows raw data from a test with 3% O_2. Because of the residence time distribution of the reactor system, the release of N, according to the measured NO signal, differs from the release of N from the particle. For this reason, the measured signal was deconvolved using the residence time distribution based on a step response test. Figure 2 shows two distinct behaviors: (1) the first peak occurring during the first 60 seconds representing the devolatilization and (2) the slower char oxidation stage. In the present study, only the char oxidation stage is considered. All experiments were repeated at least two times and the repeatability was good (repetitions shown in supplementary material).

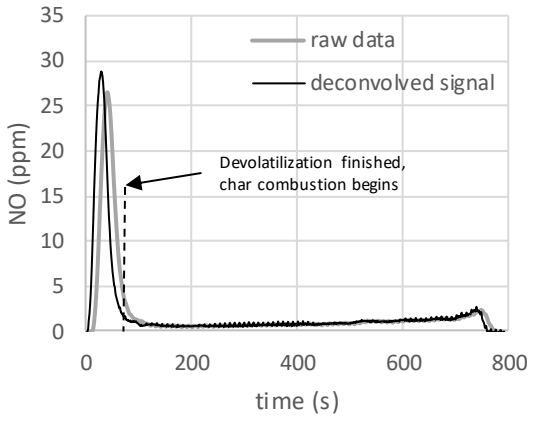

Fig. 2. NO ppm raw data from single particle reactor and deconvolved signal at 900 °C and with 3% O_2 in the gas.

2.3 Fixed bed reactor

Figure 3 shows the quartz fixed bed reactor used for NH_3 measurements from steam gasification experiments. The reactor is similar to that employed by Zhao et al [20]. Three independent heating elements ensured a uniform temperature gradient. A thermocouple, located 0.5 cm below the porous plate on which the gasification reactions took place, measured the reaction temperature. A solid feeding device allowed the admission of samples at the desired temperature and gas phase

composition in the reactor. In the experiments, 2 g of quartz sand with a size of 250-355 µm, treated at 800°C, was added together with 100 mg of char samples to ensure plug flow through the bed and facilitate the sample admission. The chars for the fixed bed experiments were produced at 900 °C in 100% N_2. Blank tests revealed that the treated sand resulted in no release of NH_3. The experiments were conducted at 900 °C with 3% steam in the gas. NH_3 concentrations of product gases were continuously measured with an ABB AO2020 Analyzer (Limas11 HW). The measuring range for the NH_3 analyzer is 0-1000 ppm. The accuracy of the NH_3 analyzer < 2% of the measurement range.

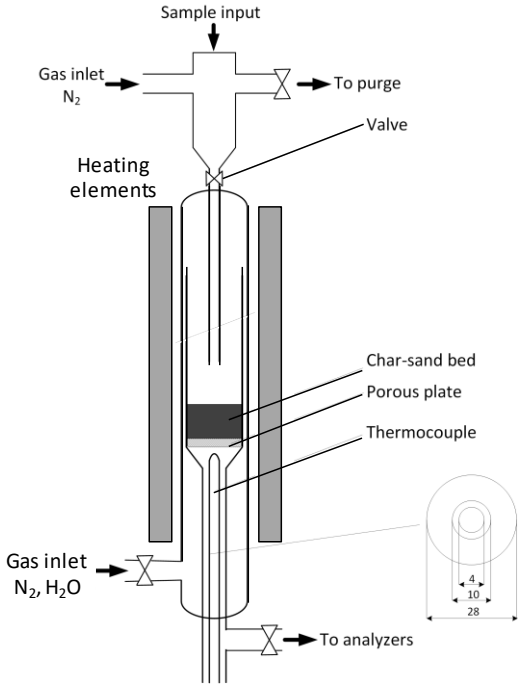

Fig. 3. Fixed bed reactor for steam gasification and NH_3 measurements [20].

2.4 Split of N in char and volatiles

The N contents of the parent fuel and char were 0.27 and 0.32 wt.%, respectively. The N content of the char was 0.08 wt.% on initial fuel basis (0.32 wt.% x 0.249) and the N content of the volatile matter was 0.19 wt.% on initial fuel basis. Thus, the split vol-N/char-N was 70%/30%.

3. Results and Discussion

3.1 Conversion of char-N to NO

Figure 4 shows experimental NO concentrations during the combustion in 3 % O_2 and in 3% O_2/14% H_2O. The char conversion occurs more rapidly in 3% O_2/14% H_2O than in 3% O_2. This can be explained by the rapid char gasification rates in the presence of H_2O. Single particle tests were also done without O_2 and with 14% H_2O. In these tests NO was not observed during the char gasification. The total conversion time (not shown here), including devolatilization, based on measured CO and CO_2 concentrations was around 500 seconds in 0% O2/14% H_2O, as compared to 370 seconds in 3% O2/14% H_2O, and 750 seconds in 3% O_2/0% H_2O. The rapid carbon conversion rates in steam can be explained by the presence of catalytic elements, i.e., K and Ca (see table 2) [21,22].

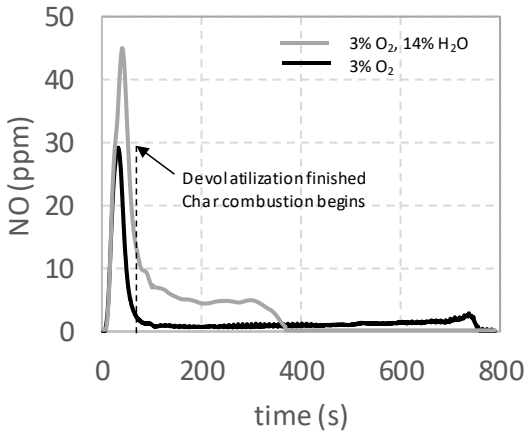

Fig. 4. NO versus time in O_2 and in O_2/H_2O from a single particle combustion tests of spruce bark at 900 °C.

The NO levels during the char conversion stage are significantly higher when steam is present in the gas. To determine the amounts of nitrogen released as NO during the char conversion, the measured curves were integrated and recalculated to amounts of nitrogen based on the total flow through the reactor. In Fig. 4, around 15% of the char-N formed NO in the case without steam, while almost 30% of the char-N formed NO in the case with steam. Figure 5 shows the amounts of N released as NO for the six different cases. In all cases, the amounts of N released as NO are significantly higher with steam

present in the gas. To the authors' knowledge, the influence of steam on the NO release has not been observed previously. Different trends regarding the conversion of fuel-N to NO may be observed in the cases with and without steam in the gas. In the case without steam, the conversion of char-N to NO increases with increased O_2 concentration, while in the case with steam, the conversion of char-N to NO decreases with increased O_2 concentration**.** In the different cases, 3-8 % of the initial fuel-N (around 10-30% of the char-N) is released as NO during the char combustion stage. The conversion of char-N to NO has been found to be lower, in general, than 50% in environments of O_2/N_2 [2,9,10,18,19,23]. In a few cases conversions of char-N to NO as high as 70% have been reported [10,19].

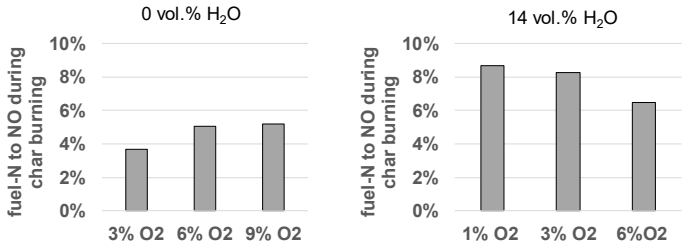

Fig. 5. Amounts of N released as NO during char combustion from single spruce bark pellets at 900 °C with and without H_2O in the gas.

In Fig. 4, the shapes of the NO release curves differ during the char combustion stage. In O_2/N_2, the NO release increases throughout the char conversion. This has been observed in previous studies and can be explained by the fact that as the char is consumed and the char particle decreases in size, there is less possibility for initially formed NO to be reduced to N_2 [7-11]. This interesting trend cannot be observed for the char conversion in $O_2/H_2O/N_2$. One explanation for this is that the char-N is not initially forming NO, but instead an NO precursor, so that the heterogeneous NO reduction step is eliminated.

3.2 Influence of H_2O and O_2 on char conversion

The oxidation of carbon and nitrogen has been assumed to be non-selective for coal chars [7,8,24,25], with some exceptions [26,27]. The relative contributions of H_2O, O_2 and CO_2 on the conversion of biomass char-N have not been investigated. This is a difficult task, as the reactions of char-N are side reactions: the main reactions are the ones with char-C. In fact, the relative contributions of H_2O, O_2

159 and CO_2 on char-C conversion in biomass combustion has not been investigated in detail. At
160 sufficiently low temperatures, O_2 is the primary gaseous reactant, but as the temperature increases,
161 also CO_2 and H_2O oxidize the char-C. For coal chars, H_2O and CO_2 play an important role in oxidizing the
162 carbon at very high temperatures such as in pulverized fuel combustion. Stanmore and Visona [28]
163 showed that, for pulverized coal char particles, H_2O and CO_2 can contribute to char conversion already
164 at 1200 °C. Based on Fig. 4, it is obvious that steam strongly contributes to the conversion of the
165 investigated biomass char at 900 °C.

166 In order to determine the relative contributions of H_2O and O_2 a detailed single particle model was
167 used [29]. The model equations and assumptions for the modeling are available in the supplementary
168 material. The single particle model takes into consideration homogeneous chemistry and temperature
169 gradients in the boundary layer of the particle. The reactions between O_2 and char-C are assumed mass
170 transfer limited. Kinetic parameters for steam gasification reactions were determined by fitting
171 computed char gasification times to experimentally determined char gasification times at 900 °C in
172 H_2O/N_2.

173 Figure 6 shows computed concentrations of the main gaseous species inside the particle and in the
174 boundary layer of the particle combusted in 3% O_2/14% H_2O. These computations were done to
175 investigate the contribution of steam gasification in the single particle reactor experiments. The same
176 particle size, i.e. 8 mm, is used as in the experiments. It can be seen that little O_2 reaches the particle
177 surface, which is expected since the O_2 oxidation reactions are assumed mass transfer limited, and O_2
178 is consumed in the boundary layer of the particle. Significant steam concentration gradients are
179 present inside the particle, emphasizing the conversion of char-C by steam. Also, relatively high
180 concentrations of CO_2 are present inside the particle, although the combustion occurs in an $O_2/H_2O/N_2$
181 mixture. This can be explained by the fact that steam reacts with char, producing H_2 and CO. In the
182 boundary layer of the particle the CO reacts to CO_2, consuming O_2. The formed CO_2 can diffuse back to
183 the char particle and gasify the char carbon. Thus, also CO_2 contributes to the consumption of char-C.

Park et al. [12] suggested that CO_2 reacts with char-N of coal to form N_2. This reaction has to the authors' knowledge not been investigated for biomass chars and is out of the scope of the present study.

Figure 7 shows the relative contribution of H_2O, CO_2 and O_2 on the conversion of char-C. These computations show that 75% of the char-C has been consumed by H_2O, 22% by CO_2 and only 3% by O_2. Similar calculations have previously been done for char-C of coal under pulverized fuel combustion conditions [30]. The results of the present study imply that the most of char-C consumption is due to steam gasification. Thus, by assuming that the conversion of carbon and nitrogen is non-selective; the dominant species for converting the char-N in $O_2/H_2O/N_2$ is steam. It should be noted that it is possible that also CO2 influence the conversion of char-N. In Fig. 6 it can be seen that the concentration of H_2 is significantly lower than of CO inside the particle. This can be explained by the fact that the diffusion coefficient of H_2 is significantly higher than of CO in the gas mixture. In the simulations, only one particle size was considered. It can be expected that as the particle size decreases, the relative role of oxygen increases, while the relative roles of CO_2 and steam on the char conversion decrease. For so low temperatures and small particle sizes, that only O_2, and not H_2O and CO_2, would oxidize the char it is plausible that H_2O would not influence the conversion of char-N to NO.

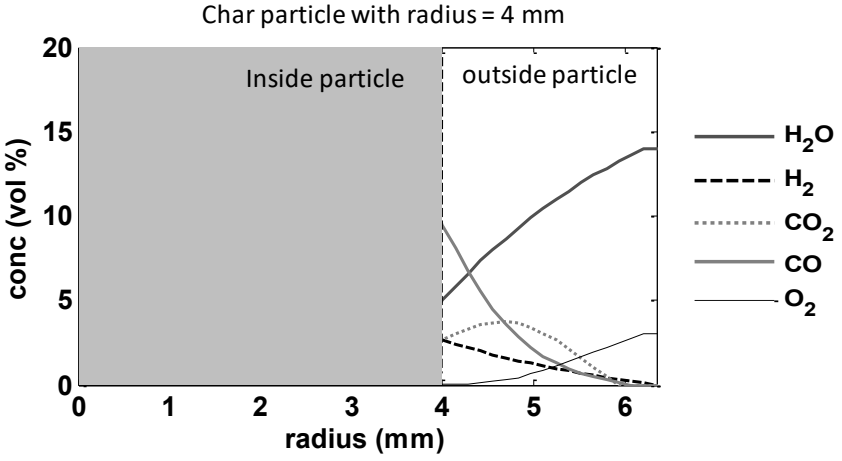

Fig. 6. Concentration profiles of H_2O, H_2, CO, CO_2 and O_2 during single particle char combustion in a mixture with 3% O_2 and 14% H_2O at 900 °C.

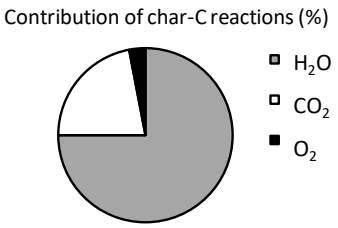

Fig. 7. Relative role of char-C oxidation by H_2O, CO_2 and O_2 during single particle char combustion in a mixture with 3% O_2 and 14% H_2O at 900 °C.

3.3 Heterogeneous chemistry: formation of NH_3

Fixed bed experiments were conducted to investigate the influence of steam on char-N. Figure 8 shows measured NH_3 concentration in product gases from steam gasification experiments of bark char. It can be seen that significant amounts of NH_3 are detected in the product gases experiments. The data shown is unfiltered explaining the noise. By integrating the measured concentrations of NH_3 and based on the total gas flow, the amounts of N were determined.

Fig. 9 shows the nitrogen contents of the char as determined from elemental analysis and as determined from NH_3 measurements based on five repeated steam gasification tests. The average N content, based on the NH_3 corresponds well to the elemental N content, implying that the char-N reacts entirely to NH_3. For coal chars it has been suggested that around 50% of the char-N forms NH_3 under steam gasification [12].

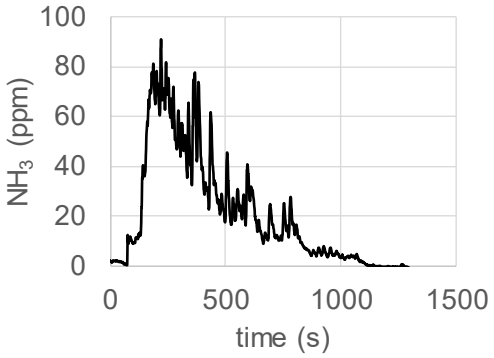

Fig. 8. NH_3 as a function of time from fixed bed steam gasification of biomass char at 900 C with 3% H_2O in the gas.

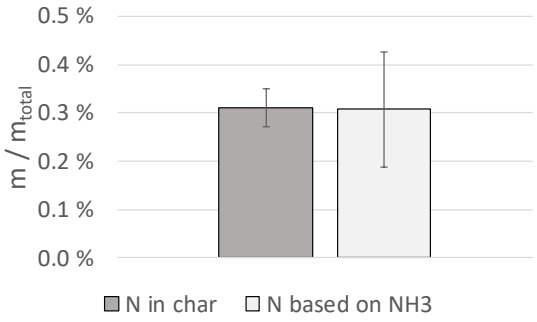

222

223 Fig. 9. N contents of char based on elemental analysis and based on measured NH_3 concentrations
224 from fixed bed steam gasification experiments at 900 °C.

225

226 **3.4 Homogeneous chemistry: oxidation of NH_3 to NO**

227 The results of Fig. 8 and Fig. 9 show that NH_3 is the main reaction product from steam gasification of
228 the investigated biomass char. It may be expected that HCN, which was not measured, is also a reaction
229 product. To investigate the influence of NH_3 on NO formation in the combustion tests, the following
230 was done to model the homogeneous reactions of the flue gas: a detailed kinetic mechanism,
231 comprising 353 reactions, was used to compute conversion of NH_3 to NO [31]. The following was
232 assumed in the modeling: (1) an isothermal plug flow reactor with a temperature of 900 °C; (2) a gas
233 mixture with initial concentrations of 13.5% H_2O, 0.5%H_2, 0.5% CO, 2.5% O_2 and 5 ppm NH_3, with N_2 as
234 the balance gas. The initial concentrations were selected in the following way: the NH_3 concentration
235 was selected based on a typical value of the measured NO concentration in the single particle tests;
236 the CO concentration was selected based on a typical value of the measured CO_2 concentration in the
237 single particle tests; and the H_2 concentration was assumed to be the same as the CO concentration
238 which can be justified by that the steam gasification reaction $H_2O + C(s) \rightarrow CO + H_2$.

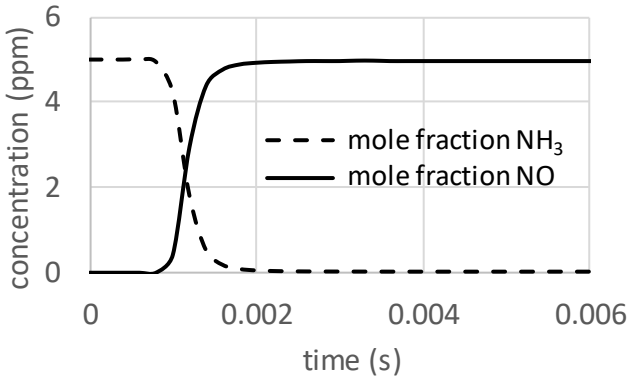

Fig. 10. Conversion of NH_3 to NO using detailed N chemistry mechanism isothermally at 900 °C, assuming the following initial concentrations: 13.5% H_2O, 0.5%H_2, 0.5% CO, 2.5% O_2 and 5 ppm NH_3.

Figure 10 plots the conversion of NH_3 to NO using the detailed N chemistry mechanism. Under the investigated conditions, the NH_3 reacts entirely to NO in less than 0.002s. The residence time in the single particle reactor, from the particle to the outlet of the reactor (this section of the reactor is heated), is around 1s, thus, several magnitudes higher than the time needed to oxidize NH_3 to NO based on the detailed kinetic mechanism. The kinetic simulations were repeated with initial values of NO between 0 and 2ppm, H_2 between 0 and 0.5%, CO between 0 and 0.5%, and CO_2 between 0 and 0.2%. In each of these simulations, the NH_3 reacts entirely to NO. Note that these simulations were done to investigate the extent to which NH_3 reacts to NO in the single particle tests of the present study. These simulations imply that NH_3 reacts entirely to NO under the investigated conditions. In industrial thermal conversion systems, NH_3 is used to reduce the NO to N_2. Such a reduction is not occurring for the given gas mixture due to the low levels of NH_3 and NO.

3.5 Influence of steam on NO release

One explanation for the higher formation of NO during char combustion in $H_2O/O_2/N_2$ than in O_2/N_2 is that steam influences the conversion of char-N. The char-N reacts to NH_3, which reacts to NO. If NO is formed sufficiently far outside the char particle surface, then the NO cannot be reduced inside the pore structure of the particle. Since little O_2 reaches the particle surface, it is plausible that the oxidation of NH_3 occurs outside the char particle. On the other hand, when steam is not present in the

reactant gas, the char-N reacts with O_2 to NO, which can partly be reduced to N_2 inside the pore structure of the particle. Thus, with steam present in the reactant gas, the final conversion of char-N to NO is higher.

3.6 Implications

Previous studies have suggested that most NOx emissions results from fuel-N released to NOx precursors during the devolatilization stage (e.g. [2,13]). While this conclusion may be valid, it is likely in some cases that also the conversion of char-N influence the NOx emissions. The results of the present study show that the NO formation during the char combustion stage differs dependent on whether there is steam present or not. In every combustion and gasification system, steam is present to some extent. Thus, when investigating the NO formation during devolatilization and char combustion, the influence of steam should be taken into consideration.

Little information is available in the literature regarding the behavior of fuel-N in industrial-scale systems. Vainio et al. [32] conducted an experimental measurement campaign in a 107 MWth bubbling fluidized bed firing bark. They measured NO, NH_3 and HCN in various vertical positions of the reactor. One of the measurement points was 2m above the bed. They found that, in that height of the reactor, the nitrogen present as NO, NH_3 and HCN corresponded to 96% of the fuel-N. The observed NH_3 concentrations were very high, i.e., almost 70% of the fuel-N had reacted to NH_3, strongly influencing the final NOx emissions. In this position almost no O_2 could be observed, suggesting that all O_2 of the primary air through the bed had been consumed. In addition, relatively low concentrations of CO_2 were observed in this position. On the other hand, the steam concentration of the gas was approximately 30%. This can be explained by the bark which had a very high moisture content of 60 wt.%. With such a high steam concentration in the flue gas, it is possible that the char was gasified by steam, to a significant extent, and that also the char-N reacted with steam to NH_3, based on the results of the present study. This may help to explain why the NH_3 concentration in the primary combustion zone of the fluidized bed was so high. In addition, if steam gasification reactions influenced the conversion of

285 char-N in the fluidized bed described above, then also the moisture content of the fuel influenced the
286 nitrogen release, since the cause for the high steam concentration in the primary combustion zone
287 was the high moisture content of the fuel. More work needs to be done on whether the fuel moisture
288 content can have an influence on NOx emissions in combustion and gasification.

289 **4. Conclusions**

290 The following conclusions can be drawn from the present study:

291 • Char-N of the investigated biomass reacted with steam forming NH_3, while NO was not
292 observed as a reaction product.
293 • In single char particle experiments, significantly more NO was formed in mixtures of $H_2O/O_2/N_2$
294 than in O_2/N_2. This can be explained by the following: (1) in O_2/N_2, char-N forms NO, which is
295 partly reduced inside the pore structure to N_2; (2) in $H_2O/O_2/N_2$, char-N reacts partly with H_2O
296 to NH_3. This NH_3 oxidizes to NO outside the char particle and cannot be reduced by the char
297 surface, resulting in higher NO release. Thus, the heterogeneous NO reduction step is
298 eliminated in the presence of H_2O. These results were supported by results from single particle
299 modeling and chemical kinetics modeling of the homogeneous chemistry.

300 **Acknowledgement**

301 This study was financed by the Academy of Finland financed project with no. 289666 – Fate of
302 Fuel Bound Nitrogen in Biomass Gasification. The staff at Technical University of Denmark is
303 greatly acknowledged.

304 **References**

305 [1] Glarborg P, Jensen AD, Johnsson JE. Fuel nitrogen conversion in solid fuel systems. Progress Energy
306 Combust Sci 2003;29:89–113.
307 [2] Konttinen J, Kallio S, Hupa M, Winter F. NO formation tendency characterization for solid fuels in
308 fluidized beds. Fuel 2013;108:238–46.

309 [3] Lane D J, Ashman P J, Zevenhoven M, Hupa M, van Eyk P J, de Nys R, Karlström O, D. M. Lewis.
310 Combustion Behavior of Algal Biomass: Carbon Release, Nitrogen Release, and Char Reactivity. Energy
311 Fuels 2014:28:41–51.
312 [4] Hupa M, Karlström O, Vaino E. Biomass combustion technology development –It is all about
313 chemical details. Proceedings Combust Institute 2017; 36: 113–134.
314 [5] Vähä-Savo N. Behavior of black liquor nitrogen in combustion: formation of cyanate. Doctoral
315 thesis. Åbo Akademi University 2014.
316 [6] Yu QZ, Brage C, Chen GX, Sjöström K. The fate of fuel-nitrogen during gasification of biomass in a
317 pressurised fluidised bed gasifier. Fuel 86 (2007) 611–618.
318 [7] Song YH, Beer JM, Sarofim AF. Oxidation and devolatilization of nitrogen in coal char. Combust Sci
319 Techn 1982; 28: 177–183.
320 [8] De Soete GG. Heterogenous N2O and NO formation from bound nitrogen atoms during coal char
321 combustion. Proceedings Combust Institute 1990;23:1257–1264.
322 [9] Karlström O, Brink A, Hupa M. Biomass char nitrogen oxidation - single particle model. Energy Fuels
323 2013;27:1410–1418.
324 [10] Karlström O, Brink A, Hupa M. Time dependent production of NO from combustion of large
325 biomass char particles. Fuel 2012; 103:524–532.
326 [11] Saastamoinen JJ, Taipale R. NOx formation in grate combustion of wood. Clean Air 2003;4:239–
327 67.
328 [12] Park DC, Day SJ, Nelson PF. Nitrogen release during reaction of coal char with O2, CO2 and H2O.
329 Proceedings combust institute 2005;30:2169–2175.
330 [13] Winter F, Wartha C, Hofbauer H. NO and N2O formation during combustion of wood straw, malt
331 waste and peat. Bioresource Techn 1999; 70: 39–49.
332 [14] Ren Q, Zhao C. NOx and N2O precursors (NH3 and HCN) from biomass pyrolysis: interactions
333 between amino acid and mineral matter. Applied Energy 2013; 112: 170–174.

[15] Toftegaard MB, Brix J, Jensen PA, Glarborg P, Jensen AD. Oxy-fuel combustion of solid fuels. Progress Energy Combust Sci 2010; 36: 581–625.

[16] Hecht ES, Shaddix CR. Geier M, Molina A, Haynes BS. Effects of CO2 and steam gasification reactions on the oxy-combustion of pulverized coal char. Combust Flame 2012; 159: 3437–3447.

[17] Gómez-Barea A, Leckner B. Modeling of biomass gasification in fluidized bed. Progress Energy Combust Sci 2010; 36: 444–509.

[18] Giuntoli J, de Jong W, Verkoojien AH, Piotrowska P, Zevenhoven M, Hupa M. Combustion characteristics of biomass residues and biowastes: fate of fuel nitrogen. Energy Fuels 24; 2010: 5309–5319.

[19] Karlström O, Perander M. DeMartini N, Brink A, Hupa M. Role of ash on the NO formation during char oxidation of biomass. Fuel 2017;190:274–280.

[20] Zhao K, Glarborg P, Jensen AD. NO Reduction over Biomass and Coal Char during Simultaneous Combustion. Energy Fuels 2013;27:7817–7826.

[21] Zhang Y, Ashizawa M, Kajitani S, Miura K. Proposal of a semi-empirical kinetic model to reconcile with gasification reactivity profiles of biomass chars. Fuel 2008;87:475–481.

[22] Dupont C, Jacob S, Marrakchy KO, Hognon C, Grateau M, Labalette F, Da Silva Perez D. How inorganic elements of biomass influence char steam gasification kinetics. Energy 2016; 109: 430–435.

[23] Zheng Y, Jensen AD, Glarborg P, Sendt K, Haynes BS. Heterogeneous fixation of N2: investigation of a novel mechanism for formation of NO. Proceedings Combust Inst 2009;32:1973–80.

[24] A. Molina, E. G. Eddings, D. W. Pershing, A. F. Sarofim. Char nitrogen conversion: implications to emissions from coal-fired utility boilers. Progress Energy Combust Sci 2000;26:507–531.

[25] J. M. Jones, P. M. Patterson, M. Pourkashanian, A. Williams. Approaches to modelling heterogeneous char NO formation/destruction during pulverised coal combustion. Carbon 1999;37:1545–1552.

[26] P. J. Ashman, B. S. Haynes, A. N. Buckley, P. F. Nelson. The fate of char-nitrogen in low temperature oxidation. Proceedings Combust Institute 1998;27:3069–3075.

360 [27] L. L. Baxter, R. E. Mitchell, T. H. Fletcher, R. H. Hurt. Nitrogen release during coal
361 combustion. Energy Fuels 1996;10:188–196.
362 [28] B.R. Stanmore, S.P. Visona. Combust Flame 1998;113:274–276.
363 [29] O. Karlström, A. Brink, M. Hupa. Combust flame 2015;162:788–796.
364 [30] E. S. Hecht, C. R. Shaddix, A. Molina, B. S. Haynes. Proceedings Combust Institute 2011;33:1699–
365 1706.
366 [31] Coda Zabetta, E., Hupa, M., A Detailed Kinetic Mechanism with Methanol for Simulating Biomass
367 Combustion and N-Pollutants. Combust Flame 2008;152:14–27.
368 [32] Vainio E., Brink A, Hupa M, Vesala H, Kajolinna T. Fate of Fuel Nitrogen in the Furnace of an
369 Industrial Bubbling Fluidized Bed Boiler during Combustion of Biomass Fuel Mixtures. Energy Fuels
370 2012;26:94–101.